

# Tightly Coupled Mechanistic Study of Materials in the Extreme Space Environment

D. Levin, A. van Duin, K. Rajan, and R. Sedwick

Deborah A. Levin, Penn State University, August 2012

**Introduction:** To support the multi-scale modeling of surfaces far from equilibrium we are developing a kinetic-based approach for the transport of combinations of neutrals, charged, and two-phase gaseous and particulate high energy particles to spacecraft surfaces. When we consider the contamination problems for small spacecraft using future propellants we need to consider systems that use both chemical and electric propulsion (EP). In addition, the plume chemical species for advanced green propellants will be mixtures of ions (for colloid thrusters) as well as green propellants such as HAN. Particulates as well as gaseous species will be present. Although different types of EP systems exist we have selected the ion thruster plume as a prototype system. This will be consistent with the work of Sedwick and the first step “non-chemical”, hypervelocity impacts being modeled by van Duin and measured by Rajan. There are three research aspects that we are working on to support the modeling of surfaces under extreme conditions in the space environment: (1) development of a species dependent timestep in the direct simulation Monte Carlo (DSMC) approach, (2) Particle-in-cell (PIC) numerical technique that will be compatible with the new DSMC code, and (3) water/ice condensation modeling.

**Species-dependent time steps in DSMC:** Charge exchange (CEX) reactions between beam ions and neutral atoms are an important process for understanding energy transfer between ions and neutrals in a backflow to a spacecraft surface for future dual-propulsion type systems. This process generates fast neutral atoms by collisions with the highly energetic beam ions and produces slow ions with a thermal speed. These slow ions tend to be scattered backwards to interact with the spacecraft surface. As a preliminary case we are starting with a simple, noble gas, Xe, and its ion, of concentration  $1 \times 10^{19}$  and  $1 \times 10^{16} \text{m}^{-3}$ , respectively. Ions have about O(2) higher velocity than the neutrals, so the timestep and grid cell size criteria for DSMC calculations differs greatly for each species. A single time step could be used, however, particle collision and movement routines become very inefficient. It was suggested in the work of Serikov et al<sup>1</sup> that it is still possible to maintain the close coupling between the cross-species using a multi-step algorithm. The fundamental idea is to extrapolate the impact of collisions between fast and slow species at the short time interval of the fastest species. We performed a simple study the multi-species algorithm using a mm sized cube initialized with neutrals (Xe) and ions (Xe<sup>+</sup>) at different. Temperature relaxation of the two species was observed as the species collided and it was found that the ratio of the CPU time for the multistep to the single timestep was found to be 42.8%. While this may not seem to be very large, it can be expected that this ratio will significantly increase as the complexity of the simulation increases i.e.,

inclusion of more species with greater variability in their velocities and variability in required cell sizes.

While we have not yet implemented a coupled PIC-DSMC simulation, to demonstrate results of the DSMC species dependent time step code we consider the starting condition of a small ion thruster, such as that given by van Guilder<sup>2</sup> and Hyaku et al.<sup>3</sup> Figure 1 shows the velocity along the x-direction for the Xe atoms. Although qualitatively the result looks similar to those

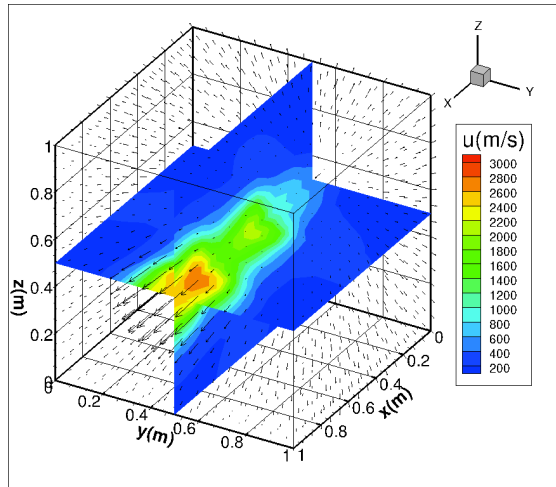


Figure 1. Neutral Xe contours using CEX reactions superimposed with velocity vectors.

that are obtained in a neutral species plume, one can observe a more complex structure which is due to CEX reactions. Ions deposit a large amount of energy into neutral, causing them to accelerate to much higher velocities compared to the neutral-only expansion. In future work we will couple these DSMC simulations with PIC to account for the affects of space-charge. As we parallelize the species time-dependent timestep code we have selected an approach that will allow us to use efficient, multi-level Octree collision grids.

#### MD Simulations of Ice formation in Space Plume

**Expansions:** We have begun molecular dynamics calculations to model formation of ice particulates from water clusters. The velocity re-scaling

technique to cool water clusters is being implemented and tested in our parallel MD code. We are working closely with Prof. van Duin's group who is using the ReaxFF model to simulate ice particle collisions with spacecraft surface materials such as Kapton. The goal of our simulations will be to create an ice formation event data base for DSMC because when "ice" formation occurs the rate of cluster growth in the plume is strongly enhanced. With our plume predictions, Prof. van Duin will simulate the correct ice-particle size and velocities impacting spacecraft surfaces to model the dusty plasma source experiments of Sedwick.

The radial pair distribution function,  $G(r)$  gives insight into how the structure of the cluster changes from gaseous to amorphous crystalline forms and the liquid state as the gas cools. Figure 2. shows a comparison between the published results of Zhang et al<sup>4</sup> and our computed results for the O-O, O-H, and H-H bonds distance distributions for a system of 256 water molecules. The published results show three curves which are calculations for amorphous ice clusters at a temperature of 70-K (bottom), and middle and top for a liquid at -30 and 75 deg-C, respectively. Hence in comparing our simulation results with their bottom curve we can see that the cooled cluster structure is very similar. Moreover, Zhang et al found that their structural calculations of water clusters agreed well with the experimental electron diffraction pattern data of Torchet et al.<sup>5</sup> This data is of interest to us because measurements were made on clusters formed in a free jet expansion, similar to the conditions of interest for our work. The

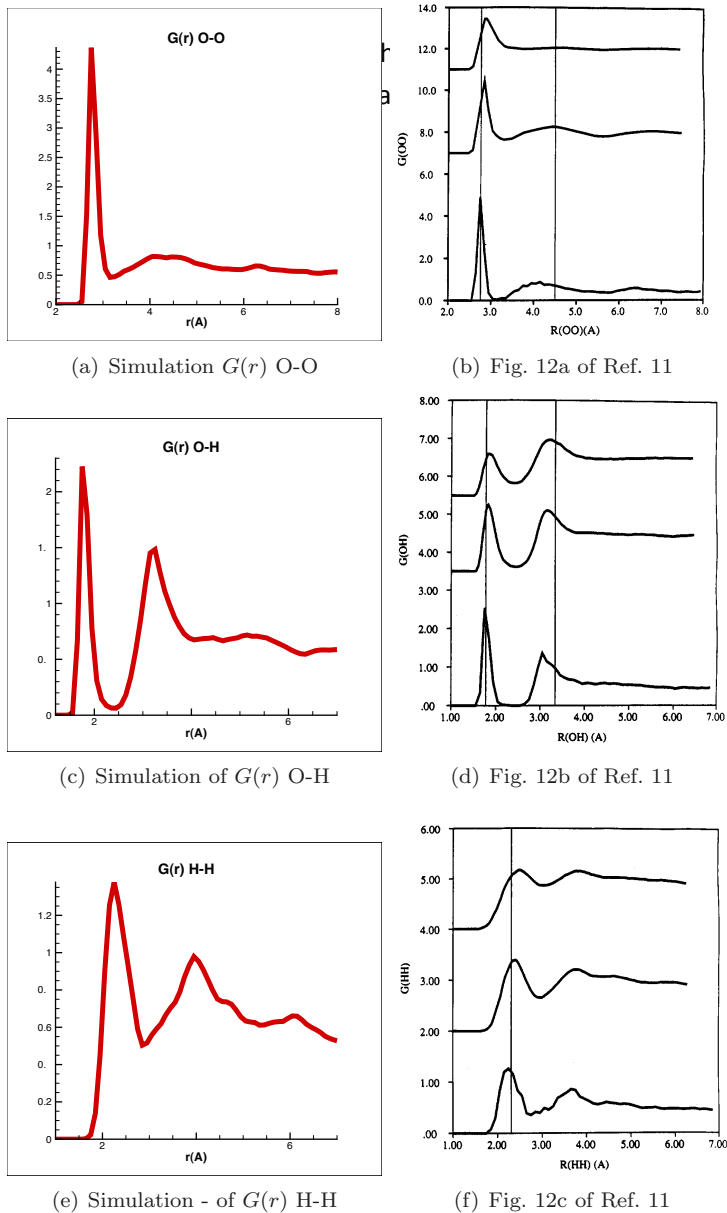


Figure 2 Comparison of simulated versus published  $G(r)$  distribution functions for a 256-water molecule cluster.

2003, Vol. 46, pp. 24-30.

<sup>4</sup>Q. Zhang and V. Buch, "Computational study of formation dynamics and structure of amorphous ice condensates", *The Journal of Chemical Physics*, Vol. 92, No. 5004, 1990.

<sup>5</sup>G. Torche, P. Schwartz, J. Farge, M. de Feraudy and B. Raoult, "Structure of solid water clusters formed in a free jet expansion", *The Journal of Chemical Physics*, Vol. 79, No. 6196, 1983.

vertical lines on the Zhang et al figures represent the location of peaks observed in the electron diffraction data. In addition to the good comparison that we find between our simulations with those of Zhang et al we can also see that in general sharper peaks in  $G(r)$  indicate more "crystalline" structure is present in the system and we can say that the conditions in which our simulations were conducted produce amorphous ice structures.

#### References:

- <sup>1</sup>V. Serikov, S. Kawamoto, and K. Nanbu, "Particle-in-Cell Plus Direct Simulation Monte Carlo (PIC-DSMC) Approach for Self-Consistent Plasma-Gas Simulations," *IEEE Transactions on Plasma Science*, 1999, pp. 1389.
- <sup>2</sup>D.B. VanGilder, "Numerical Simulations of the Plumes of Electric Propulsion Thrusters", Cornell University, 2000.
- <sup>3</sup>T. Hyakutak, M. Nishida, H. Kuninaka, and K. Toki, "DSMC-PIC Analysis of a Plume from MUSES-C Ion Engines", *Transaction of the Japan Society for Aeronautical and Space Sciences*,

Reactive molecular dynamics simulation on the disintegration of the materials used on the surface of the spacecrafts during oxygen bombardment and high energy collisions using the ReaxFF reactive force field method

A.Rahnamoun and A.C.T. van Duin, Dept. of Mechanical and Nuclear Engineering, Pennsylvania State University, August 2012

*Simulations on kapton, POSS and silica stability to oxygen bombardement.* The materials used on the surface of spacecrafts frequently collide with atomistic oxygen, especially in lower earth orbitals. These collisions cause the surface degradation of the material. In this research, atomistic scale simulation of surface degradation of kapton, POSS(Polyhedral Oligomeric Silsesquioxane)- kapton and silica, which are among the most common materials used on the surface of the spacecrafts, under collision from high energy atomistic oxygen is evaluated. The main reasons for the interest in kapton application on the spacecraft surface are the light weight, temperature stability, insulation characteristics and UV stability [1,2] of this material.

For performing these simulations, the ReaxFF reactive force field program was used, which can provide the computational speed required to perform molecular dynamics simulations on system sizes sufficiently large to describe the full chemistry of the reactions.

ReaxFF is a general bond-order-dependent force field that provides accurate descriptions of bond breaking and bond formation [3]. The main difference between traditional non-reactive force fields and ReaxFF is that in ReaxFF the connectivity is determined by bond orders calculated from interatomic distances that are updated every MD step.

After minimization and equilibration of the structures, the surfaces of these three structures are bombarded with high energy atomic oxygens. These atomic oxygens are directed towards the slabs with 4.5 eV energy. Every 200 fs time intervals, one atomistic oxygen is added to the system. The molecular dynamics simulation of these reactions are NVE simulations, indicating conservation of energy, and some key snapshots of the changes in these three slabs during the simulation are shown in figure 1. As it is shown in these snapshots, the silica structure shows the highest stability and also it is clear that changing the kapton structure to kapton-POSS structure can improve the stability of this material against high energy atomistic oxygen attack.

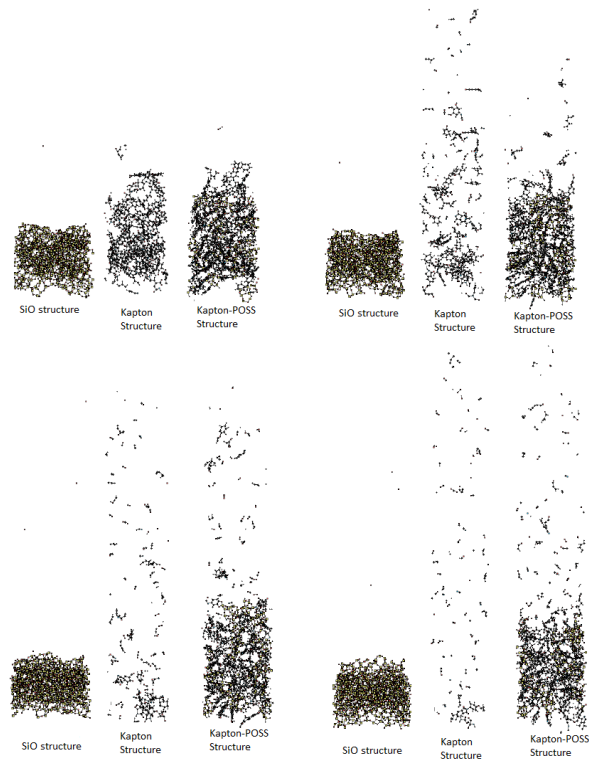


Figure 1. Key snapshots from the oxygen bombardment simulations

These simulations of Kapton, Kapton-POSS and amorphous silica subject to the high energy atomic oxygen bombardment indicate that the amorphous silica shows the highest stability

among these materials and adding Silicon to the bulk of the kapton structure enhances the stability of the structure against atomic Oxygen bombardment. Changing the Silicon content and also using other enhancement methods for kapton material like the effect of different ions additives in the bulk of kapton can enhance the stability of the kapton structure in the low earth orbital environment, but the effect of these changes on the material characteristics like brittleness should be evaluated and the best material composition should be figured out considering all the limitations. As these simulations demonstrate, ReaxFF can provide a cost effective screening tool for such material optimization.

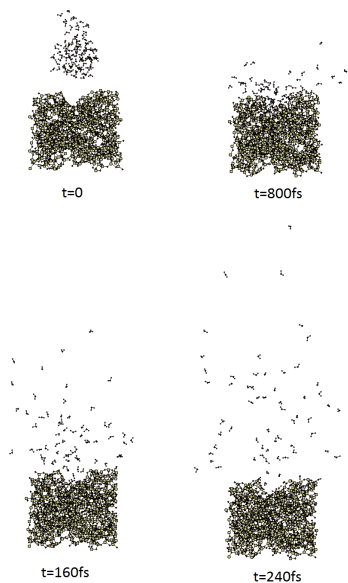


Figure 2. Key snapshots of the collision of a high velocity ice structure with amorphous silica

*Simulation on silica response to bombardment with nano-ice crystallites.* The effect of high energy collision of these materials with other species which can be present in the space, like ice and debris is another important issue which should be evaluated. Some snapshots of the collision of a high velocity ice structure with amorphous silica are shown in figure 2. The water size and structure and velocity are derived from DSMC calculations performed in Dr. Levin's group.

During the simulations, we observe that the temperature of the system decreases after the collision and this shows that endothermic reactions have taken place during the collision of the ice with silica, resulting in the formation of hydroxyl groups on the silica surface and creating of surface- and subsurface defects.

The kinetic energies of the water molecules that bounce off the amorphous silica surface after collision are shown in figure 3 at different simulation stages. The ice cluster collides the silica surface with a kinetic energy of around 240 eV. These graphs show the range of the kinetic energies of water molecules bouncing off the silica surface after the collision. Some of the water molecules, with lower kinetic energy, react with the silica surface after the collision and the number of free water molecules decreases. This information will be used by Dr. Levin's group for parameterizing their DSMC (Direct Simulation Monte Carlo) calculations for surface collision events.

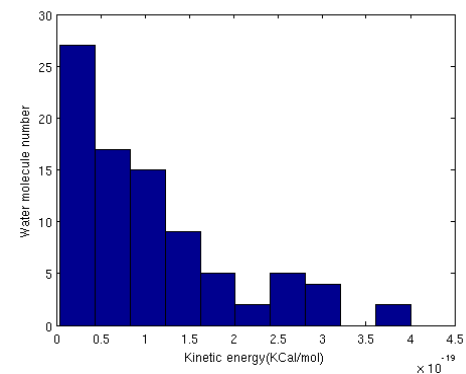


Figure 3. Kinetic energies of individual water molecules after collision with the silica slab

## References:

- [1] Tribble AC. The space environment: implementation for spacecraft design. Princeton, NJ: Princeton University Press; 1995.
- [2] Bedingfield KL, Leach RD, Alexander MB. NASA Reference Publication 1390; 1996.
- [3] van Duin et al.. *J. Phys. Chem. A* 2001, 105, 9396.

## Mechanistic Study of Materials in the Extreme Space Environment

*Krishna Rajan, Iowa State University*

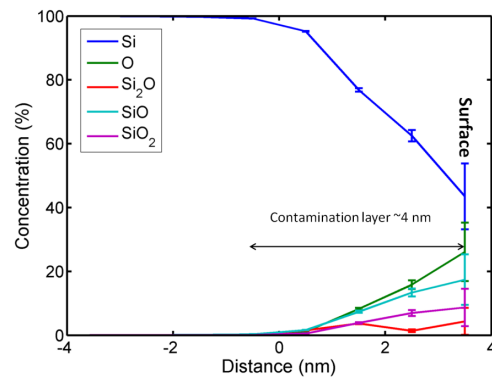
Characterization of the first few monolayers of gas-metal interaction is necessary to understand the degradation of materials under low-pressure (space) environments. During the reporting period, progress has been made in identification of nanoscale oxides and quantification of the oxide layer thickness using pulsed laser atom probe tomography (APT). (i) Measurement of gas-solid reactions by tracking degradation of the material under extreme environment conditions. (ii) Identification of surface compounds, specifically different oxidation states, formed during these gas-solid reactions. (iii) Modeling energetics of bonding during degradation and the corresponding degradation mechanism.

i) Atomistic Imaging of Nano-scale Surface Oxide: We have developed capabilities for characterizing gas-solid reactions in the atom probe coupled with atomistic scale chemical imaging. Solid-gas reactions were performed in a reaction chamber with temperature and pressure control. The temperature of a metal specimen was heated to 450 °C, and gas was inlet to a pressure of  $10^{-3}$  torr. The sample was then characterized in APT for nano-scale characterization of the surface oxides, the diffusion of oxide into metal, and the phase formations. By tracking the degradation of the material, the relative bonding between atoms is detected and the different oxidation states are identified.

### *(a) Si / Silical Oxygen Reactions*

A Si specimen was introduced to a gas environment (O) and the gas-solid reactions were measured in terms of surface compound formation and different oxidation states. The different metal-oxide surface compounds were measured and spatially resolved (cross section of data shown in Figure 1). The atoms which are shown as O are less strongly bonded to Si than the atoms which are part of a Si-O compound. The majority of the O atoms are seen on the surface, indicating that the metal-oxygen bonds at the surface are relatively weak. For cases where the gas diffused partially through the metal, the bonding between gas and metal becomes significantly stronger. Therefore, understanding the degradation of a surface after gas-solid reaction requires understanding oxidation states as a function of diffusion. Figure 2 shows a diffusion profile across the surface of the material to identify the preferred stoichiometry of silicon oxides as a function of the distance from the silicon-oxygen interface. These diffusion profiles provide information about the metal-gas reaction kinetics at the nanoscale that can be extrapolated to quantify the lifetime of a materials. The depth of ingress of oxygen (~4 nm) provides quantitative information about the thickness of the contamination layer and the bond strength of these contaminant atoms. This demonstrated ability of the APT to simultaneously image and chemically quantify gas-solid interactions at atomic level enables us to systematically quantify these interactions as a function of material chemistries and crystallographic orientations

Figure 1. Concentration profile measuring surface chemistry and the diffusion of gas into the material. The ratio of O:Si-O compounds decreases with diffusion distance, implying that the metal-gas reactions and subsequent bond strengths are strongest at the metal-gas interface, while the resulting surface atoms are more weakly bonded to material



(b) Al / Alumina/ Oxygen Reactions

The APT analysis of Al<sub>2</sub>O<sub>3</sub> reaction, which showed oxide forming in (100) direction, provides the following conclusions: (i) Interface of solid-gas reaction can be imaged and concentration profiles, compounds and valencies at the interface are identified. (ii) Oxygen diffusion is limited to the first 1.5 nm of Al, with very limited solubility of O into Al. (iii) At the interface, the Al has Al<sub>2</sub>O stoichiometry which is different than the stoichiometry of alumina at the sample surface. (iv) The Al atoms have valency of one in the bulk of the material; however, a large number of Al atoms at the interface have a valency of two. Understanding the valency as a function of surface / reaction is needed to understand the solubility occurring during potential reactions. (v) By studying the degradation mechanisms of the material, we identify not only what atoms evaporate, but what atoms evaporate together (Figure 2).

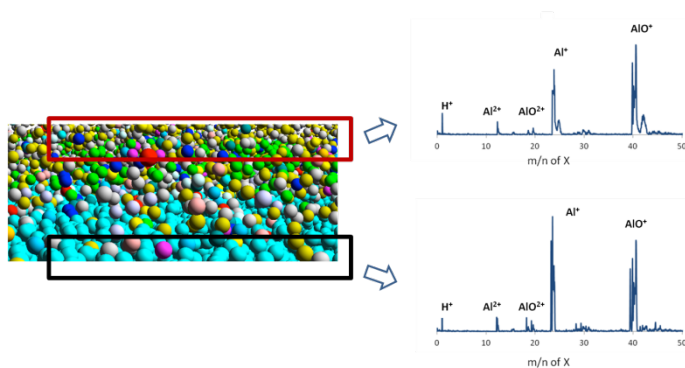


Figure 2. Characterization of pair wise interactions between Al and other atoms / compounds at the atomic scale. The top spectra describes the compounds and corresponding valencies that degrade concurrent with Al<sup>+</sup> atom in the alumina region at the interface; the bottom spectra is the same except in the Al region near the interface. This map allows us to understand the complexity of the chemical states and

identify the differences in bonding and inter-atomic interactions. The differences in the spectra represent changes in material degradation between phases at the metal surface, and describe the strength of inter-atomic interactions and mechanism for gas-solid reaction.

ii) Energetics of Materials Degradation: An atomistic based computational technique has been developed for modeling degradation mechanism of materials under extreme environment. Initial work has been done for metallic Al alloys to establish the computational robustness of the method. Future work will repeat this calculation for aluminum oxides as observed experimentally by atom probe.

# Tightly Coupled Mechanistic Study of Materials in the Extreme Space Environment

Ray Sedwick  
University of Maryland

The space environment consists of a variety of species and energy spectra, some naturally occurring and some generated by plume exhaust and space debris. A variety of plasma sources are under development or have been acquired by the UMD Space Power and Propulsion Laboratory to simulate the space environment. A mini ion engine has been developed to generate the ion energies and densities that are generated by electric propulsion systems on-orbit, allowing for the effects of plumes on neighboring spacecraft to be studied, as well as back scattered ions resulting from charge exchange processes. A Gen-II IonEtch sputter gun ion source has been acquired that can generate reactive species, such as atomic oxygen, at energies as high as 5 keV. Under a recently awarded DURIP, a dusty plasma source is being developed to study the impact of particulates on material surfaces, representative of small space debris particles.

## Plasma Sources:

### Ion Engine Simulator

One plasma environment of interest is the environment generated by the propulsion system itself. Electric propulsion systems generate energetic ion streams capable of eroding material from the outer surface of a spacecraft, which can be particularly problematic for optical surfaces or the protective coatings of solar arrays. There are two ways in which such plasma environments can affect spacecraft. The first is through interactions with other spacecraft that are flying in formation. Such architectural designs are becoming more prevalent as desired capabilities demand aperture sizes that outpace launch faring dimensions. Formation control maneuvers will frequently demand thrust profiles that will cause these high energy plumes to be directed at other vehicles in the cluster. A second way that plumes can interact is through charge exchange with low energy neutrals, resulting in low energy ions which can be drawn back to the vehicle with floats at a negative bias relative to the local plasma environment. The plasma environments that are generated in these plumes due to charge exchange (CEX) processes are being modeled using DSMC by Levin. The ion engine simulator hardware can then be used as a validation of the CEX models as discussed below. Regardless of the mechanism, the effect of the energetic ion beams on material surfaces will be experimentally determined using the ion engine simulator source, with ion energy and density as established by either common operating points (interspacecraft plume interactions) or the ion backflow due to DSMC. Specially prepared target specimens (discussed below) will be used to for a more complete assessment of the damage generated by this interaction.



**Figure 1.** Ion engine simulator with a bare filament cathode and magnetically isolated anode. Ion energies can range from 0 – 500 eV with currents up to ~10 microamps.

## Gen-II IonEtch Sputter Gun

Another source of environmental degradation at lower altitudes is through the interaction with plasmas generated in the ionosphere. Of particular interest are the reactive species such as atomic oxygen that in addition to being of sufficient energy to erode material are also like to interact chemically with the outer surface of the spacecraft, making them even more problematic. The nature of the ion engine simulator, with its filament cathode is not effective at generating reactive plasmas, since the lifetime of the filament would be substantially shortened. The IonEtch uses a microwave plasma source that is capable of generating a plasma from a greater variety of species. The gun is capable of much higher energies than would typically be encountered, but at lower energies it can generate currents up to 1 mA, better approximating the plasma environment that would be present. Modeling of the interaction of such species with spacecraft materials under this program is being conducted by van Duin, with diagnostics capable of imaging the detailed results of these interactions developed by Rajan.



**Figure 2.** Gen-II IonEtch sputter gun, capable of up to 1 mA of current and up to 5 keV beam energy. Reactive species can be generated using microwave ionization.

## Laser Ablation Dusty Plasma Source

A third source of environmental interactions are through space debris. Debris can vary from objects as large as several thousand kilograms to dust particulates. The interaction with the former will most certainly be catastrophic, but the likelihood is much lower. As the size of the debris is reduced, the likelihood of interaction grows, and at the size of dust particles that interaction is nearly continuous. Impact rates will vary with different altitudes, with impact velocities determined by orbital parameters and energies dictated by particle size. To investigate this interaction, a dusty plasma source is being developed under DURIP funds. The plasma source uses laser ablation of material to generate particles of various sizes and densities that can be characterized and selected using time of flight to impact a test article. Smaller particle sizes and their impact on material surfaces can be modeled using ReaxFF (van Duin) and compared to surface damage using a scanning electron microscope (SEM).

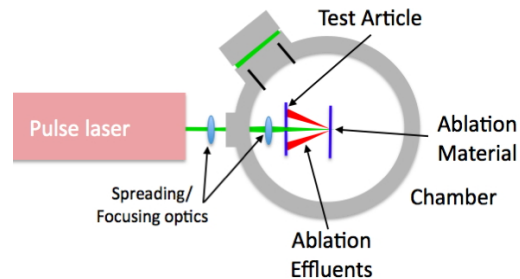


**Figure 3.** Conceptual design of dusty plasma source using laser ablation of material. Selection of pulse energy and duration will determine particle size and energy for a particular material.

## Plasma Diagnostics:

### Retarding Potential Analyzer (RPA)

The main diagnostic device used for evaluating the plasma environment is the retarding potential analyzer (RPA). Using a discriminating grid bias that reflects ions below a selectable threshold energy, the spectrum of the ion beam energy can be determined. Figure 4 (top) shows the physical layout of the RPA along with the effect of varying the grid bias on the admitted ions. The same figure (bot) shows an example of the resulting energy spectrum coming out of the ion engine simulator. This spectrum shows a peak at around 17 eV (on the low end for a plume, but possibly representative of the sheath fall for back scattered ions) with a spread in energies from as low as a few eV to as high as 30 eV. Some spread in energies will result from collisions, as well as from the CEX process, which will tend to populate the lower energies as shown. By taking measurements at different locations axially and radially through the beam, the effects of CEX can be quantified. The spectrum of ion energies is being calibrated to the engine operating parameters so that a known spectrum and fluence can be delivered to a test article.

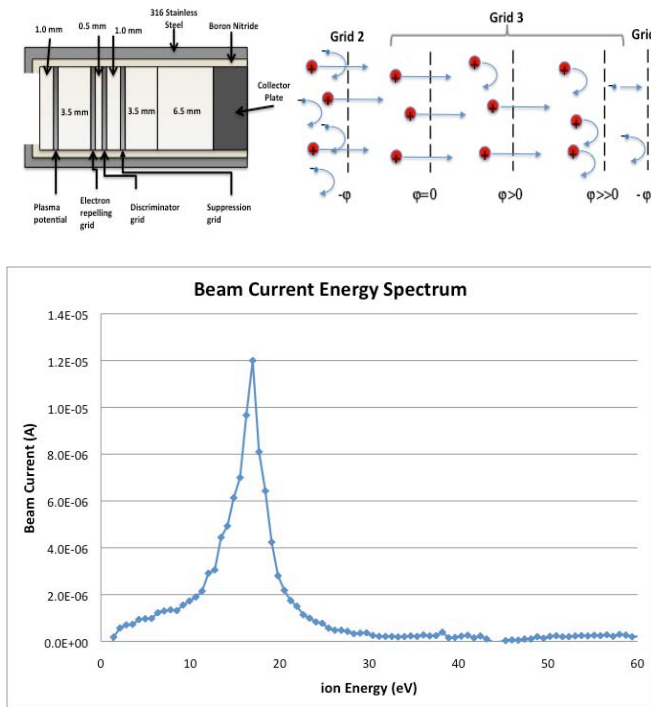


**Figure 4.** (top) RPA design showing selectivity of different ion energies at different grid biases. (bot) Beam current energy spectrum found using RPA.

## Test Articles:

### Silicon Needle Arrays

While qualitative, and even some quantitative data on material degradation can be achieved using SEM imagery, Atom Probe Tomography (Rajan) will be used to reconstruct a 3D map of needle shaped specimens subjected to the plasma environment. The needles are prepared in 6x6 arrays, currently fabricated from Silicon through an etching process on 7mm x 3 mm wafers. These are then mounted on a test support in the beam of the ion source and bombarded with ions of a specified energy until a sufficient fluence has been achieved. The coupons are then shipped back to Iowa State University where they are processed using ATP. The results can then be compared with the numerical simulations from PSU.

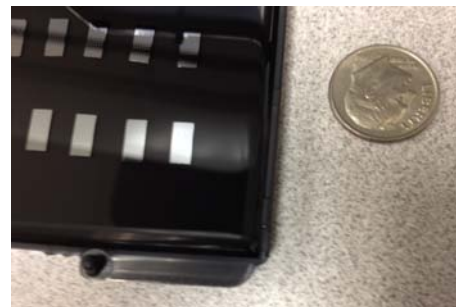


**Figure 5.** Test coupons (silver, left) each with 36 (6x6) needles, 100 microns high (+/-20%) and 50 nm in diameter.